



<b>Title</b>	<b>Dye-sensitized solar cells using ZnO tetrapods</b>
<b>Author(s)</b>	<b>Hsu, YF; Xi, YY; Yip, CT; Djuriši, AB; Chan, WK</b>
<b>Citation</b>	<b>Journal Of Applied Physics, 2008, v. 103 n. 8</b>
<b>Issued Date</b>	<b>2008</b>
<b>URL</b>	<b><a href="http://hdl.handle.net/10722/57306">http://hdl.handle.net/10722/57306</a></b>
<b>Rights</b>	<b>Journal of Applied Physics. Copyright © American Institute of Physics.</b>

## Dye-sensitized solar cells using ZnO tetrapods

Y. F. Hsu,<sup>1</sup> Y. Y. Xi,<sup>1</sup> C. T. Yip,<sup>1</sup> A. B. Djurišić,<sup>1,a)</sup> and W. K. Chan<sup>2</sup>

<sup>1</sup>*Department of Physics, The University of Hong Kong, Pokfulam Road, Hong Kong, China*

<sup>2</sup>*Department of Chemistry, The University of Hong Kong, Pokfulam Road, Hong Kong, China*

(Received 13 December 2007; accepted 22 February 2008; published online 24 April 2008)

One dimensional (1D) ZnO nanostructures are of interest for applications in dye-sensitized solar cells (DSSCs) since they exhibit significantly improved electron transport compared to that in porous films. However, 1D nanostructures also have a significantly lower surface area than the porous films. Thus, the achieved solar cell efficiencies are typically much lower in spite of the improved charge transport. In this work, we investigated DSSCs based on ZnO tetrapods to achieve an increased surface area compared to that of 1D nanostructures. The cell performance as a function of the tetrapod film thickness and the dye used was studied. To further increase the surface area, mixed morphologies (tetrapods with nanoparticles) were also investigated. Under optimal conditions, an AM 1.5 power conversion efficiency of  $\sim 1.2\%$  was achieved. © 2008 American Institute of Physics. [DOI: 10.1063/1.2909907]

### I. INTRODUCTION

Since titanium dioxide (TiO<sub>2</sub>) based dye-sensitized solar cells (DSSCs) were reported by O'Regan and Grätzel in 1991,<sup>1</sup> a lot of work has been done in trying to improve their performance. A DSSC typically consists of a porous layer composed of TiO<sub>2</sub> nanoparticles. Under illumination, the dye absorbs the light and the dye excited states undergo charge separation. Electrons are injected into the porous oxide film and the dye is regenerated by electron donation from the electrolyte, which is usually an organic solvent containing a redox system.<sup>2</sup> Electron transport in that case is by trap-mediated diffusion, which is a slow mechanism.<sup>3</sup> Therefore, alternatives, such as TiO<sub>2</sub> single crystalline nanowires and other metal oxide materials, are investigated in order to achieve a faster electron transport and, thus, improve the efficiency.<sup>4-6</sup>

Zinc oxide, which has a high mobility on the order of 100 cm<sup>2</sup>/V s, is thought to be a potential substitute for TiO<sub>2</sub> due to their similar band gaps and electron affinities. It has an additional advantage over TiO<sub>2</sub> in that greater varieties in morphologies with a large surface area can be fabricated, which is an essential factor in maximizing dye adsorption. However, the energy conversion efficiency of ZnO based cells sensitized by ruthenium dyes is typically not as high as that of cells that use TiO<sub>2</sub>, although some examples of ZnO based cells sensitized by a different dye with a good efficiency (2.4%) were reported.<sup>7</sup> Therefore, there is considerable interest in further improving the morphology of a ZnO photoanode in order to simultaneously achieve a high surface area and an efficient charge transport and, thus, improve the efficiency of ZnO based cells. One possible method to increase the surface area is to use branched structures instead of one dimensional nanowires. It was reported that hyperbranched nanocrystal-polymer solar cells have a higher efficiency than nanorod-polymer solar cells because the branching structure could provide a large surface area for charge

separation.<sup>8</sup> Tetrapods, which have four legs extending from a common core, are expected to result in solar cells with a higher efficiency due to their large surface area. In addition, they can be easily attached onto a substrate layer by layer as well as mixed with other ZnO nanostructures by using simple methods. Hence, the surface area used to adsorb dye can be significantly increased, resulting in an increased absorbance and, consequently, a higher short-circuit current density.

Thus, we have prepared ZnO tetrapod film based solar cells for different film thicknesses and studied their photovoltaic performance. The effect of different sensitizers, such as N3, N719, and mercurochrome, on the cell performance was also studied since it was shown that a low cost dye such as mercurochrome can be an efficient sensitizer for ZnO.<sup>9</sup> Finally, ZnO nanoparticles were added to the tetrapods to further increase the surface area. The highest achieved efficiency was  $\sim 1.2\%$ .

### II. EXPERIMENTAL DETAILS

Tetrapods were fabricated from 0.2 g zinc powder (Aldrich, 99.995%) under the flow of 0.2 l/m humid argon gas at 950 °C, as described in detail elsewhere.<sup>10</sup> The morphology of the tetrapods was characterized by scanning electron microscopy (SEM) by using a Leo 1530 field emission SEM. To prepare the tetrapod film, the tetrapod powder was mixed with a 0.25M zinc acetate/ethanol solution and spin coated on indium tin oxide coated glass sheets (ITO/glass) at 500 rpm. The whole assembly was heated to 200 °C at a rate of 5 °C/min, annealed for 20 min, and then cooled down to room temperature at a rate of 1 °C/min. This process was repeated several times depending on the desired thickness. To further increase the surface area for dye adsorption, ZnO nanoparticles (Nanoscale Materials, Inc.) were also dispersed into the zinc acetate and tetrapod/ethanol solution, with the ratio of the nanoparticles to tetrapods of 1 to 2. According to the manufacturer's specifications, the nanoparticles had a crystallite size of  $\sim 10$  nm and formed aggregates of

<sup>a)</sup>Electronic mail: dalek@hkusua.hku.hk.

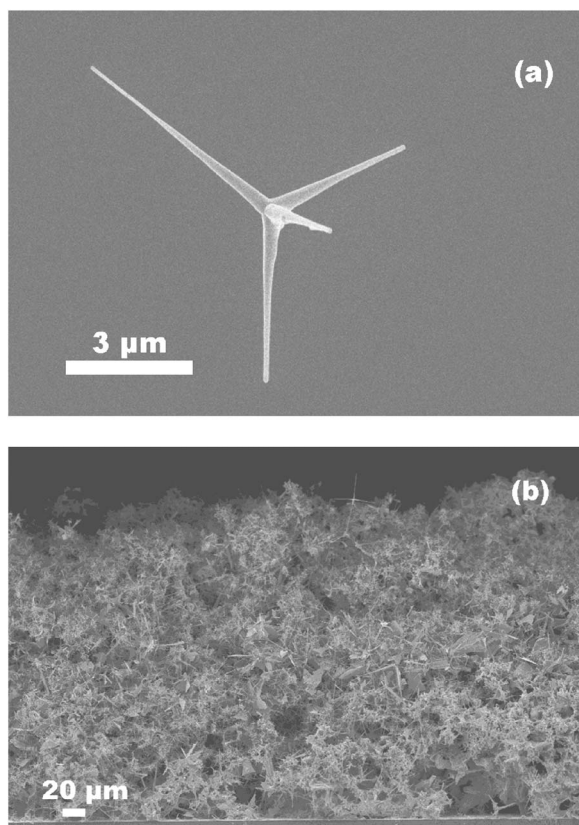


FIG. 1. Representative SEM images of (a) a tetrapod and (b) tetrapods attached to ITO/glass that were used to fabricate DSSCs.

$\sim 4 \mu\text{m}$ , which has been verified by transmission electron microscopy. The mixed solution was then spin coated and the samples were annealed. The thickness was determined by means of SEM (Leo 1530 field emission SEM). The samples were immersed either into a 5 mM ethanolic solution of *cis*-bis(isothiocyanato) bis(2,2'-bipyridyl-4,4'-dicarboxylato) ruthenium(II) bis-tetrabutylammonium (N719) (Solaronix), *cis*-di(thiocyanato)-*N,N*-bis(2,2'-bipyridyl dicarboxylate) ruthenium(II) (N3) (Solaronix), or mercury dibromofluorescein disodium salt (mercurochrome) (Aldrich), which were kept at  $80^\circ\text{C}$  for 2 h. The solar cells were assembled by using an Iodolyte R-150 electrolyte (Solaronix) and a platinum coated conductive oxide glass as a counterelectrode (Solaronix), and the  $I$ - $V$  relationship of the cell was measured by a Keithley 2400 sourcemeter under the illumination of an Oriel 66002 solar light simulator (AM 1.5,  $100 \text{ mW cm}^{-2}$ ). The active electrode area was  $0.385 \text{ cm}^2$ . The efficiencies  $\eta$  of the solar cells were calculated as

$$\eta = \frac{V_{\text{oc}} J_{\text{sc}} \text{FF}}{P_{\text{in}}}, \quad (1)$$

where  $V_{\text{oc}}$  is the open-circuit voltage,  $J_{\text{sc}}$  is the short-circuit current density, FF is the fill factor, and  $P_{\text{in}}$  is the optical power.

### III. RESULTS AND DISCUSSION

Representative SEM images of an individual tetrapod and an assembly of tetrapods on the ITO/glass are shown in Fig. 1. A tetrapod has four legs extending from a common

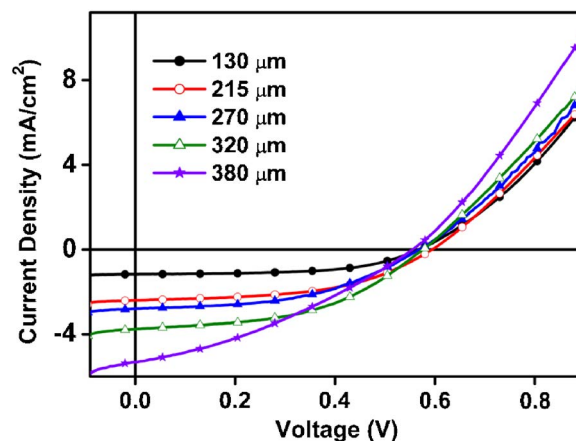


FIG. 2. (Color online) Photocurrent-voltage characteristics with different tetrapod layer thicknesses.

core. The length of the tetrapod legs is dependent on the substrate temperature, so that tetrapods with leg lengths within the range of  $1\text{--}20 \mu\text{m}$  are obtained. It can be observed that the tetrapods can connect with each other and form a porous network. Figure 2 and Table I show the cell performance for different tetrapod film thicknesses. It should be noted that for thicknesses  $\leq 215 \mu\text{m}$ , the FF remains  $\geq 0.50$ , indicating that the tetrapod network exhibits efficient electron transport. For comparison, cells based on  $20 \mu\text{m}$  long ZnO nanowires exhibited a significantly lower FF, FF =  $0.36\text{--}0.38$ .<sup>5</sup> The increase in thickness of the tetrapod film resulted in an increase in  $J_{\text{sc}}$ , but at the same time, FF decreased. This was due to the presence of more tetrapods, leading to an enhancement in the surface area for dye adsorption and, consequently, increasing  $J_{\text{sc}}$ . However, a larger surface area added the number of recombination sites, thus decreasing FF, which was affected by the recombination loss.<sup>11</sup> Moreover, the increase in thickness increased the resistance of a cell, which also contributed to the decrease in FF. Nevertheless, the overall efficiency could be improved by a higher adsorption area of the dye as  $J_{\text{sc}}$  more significantly increased than FF, but it would reach a saturation value, just as in the case of ZnO nanoparticle based DSSCs, although the saturation for tetrapods occurs at a considerably higher film thickness compared to that of nanoparticles.<sup>12</sup>

In addition to the large surface area, the dye used is another very important factor that can affect the performance of the cells. Ruthenium dye N3 is commonly used in  $\text{TiO}_2$  based DSSCs. The main anchoring group of this kind of dye molecule is the carboxyl group, which can strongly adsorb

TABLE I. Performance of the cells with different thicknesses of the tetrapod film.

Thickness ( $\mu\text{m}$ )	$J_{\text{sc}}$ ( $\text{mA/cm}^2$ )	$V_{\text{oc}}$ (V)	FF	Efficiency (%)
130	1.17	0.59	0.56	0.39
215	2.40	0.595	0.50	0.71
270	2.80	0.57	0.47	0.75
320	3.76	0.58	0.47	1.02
380	5.33	0.56	0.33	0.98



TABLE II. Performance of the cells with different kinds of dye.

Dye	$J_{sc}$ (mA/cm <sup>2</sup> )	$V_{oc}$ (V)	FF	Efficiency (%)
N3	1.36	0.58	0.40	0.32
N719	1.17	0.59	0.56	0.39
Mercurochrome	1.34	0.54	0.49	0.35

onto the metal oxide surfaces. In ZnO based DSSCs, the sensitization process involves the diffusion of the dye among the ZnO nanostructures, adsorption of the dye onto the ZnO surface, dissolution of the Zn surface atoms from ZnO, and the formation of Zn<sup>2+</sup>/dye complexes in the pores when the dye molecules reach the interface between the back contact and the ZnO film. The formation of metal-ion/dye complexes does not take place in TiO<sub>2</sub>, but it is very significant in ZnO.<sup>13</sup> Protons derived from Ru complexes make the dye-loading solution relatively acidic and dissolve ZnO, generating Zn<sup>2+</sup>/dye aggregates, which are harmful to the ZnO DSSC performance because they lower electron injection efficiencies and fill the pores of ZnO photoanodes.<sup>14</sup> This problem can be solved by using an unprotonated dye or a more basic dye solution. Therefore, N719 is usually used as a sensitizer in ZnO solar cells instead of the commonly used N3 dye.<sup>15</sup>

In this work, the influence of the dye used on the performance of the cells was studied. The obtained results are summarized in Table II. It can be observed that the cells with N719 as a dye had a higher efficiency than those that used N3, which is in agreement with previous studies on ZnO based cells.<sup>16</sup> In addition to N3 and N719, which are commonly used in DSSCs, cells that use mercurochrome dye have been fabricated since it has been shown that mercurochrome, which is an inexpensive common dye, yields a better performance in ZnO based cells compared to those that use N3 dye.<sup>17</sup> The tetrapod cells that used N3 as a dye had the poorest performance among the three, which was consistent with the previous studies.<sup>16,17</sup> Lower  $V_{oc}$  and FF resulted in a lower efficiency for the mercurochrome-sensitized cell compared to that of the N719-sensitized cell, but it was still higher than that of the N3-sensitized solar cell, which might be attributed to the fewer electron interfacial recombination losses and lower trap density.<sup>17</sup> For experimental conditions for the dye loading used (2 h immersion in the dye solution), the differences in the performances achieved with the three dyes were not very significant. Still, since N719 resulted in the highest  $J_{sc}$ , we used N719 to further study the effect of the surface area.

To increase the efficiency of the DSSCs, ZnO nanoparticles were also added into the tetrapod film to further increase the surface area. Figure 3 shows the SEM image of the mixed morphology film. It can be observed that nanoparticle aggregates fill the space between the tetrapods, providing an increased surface area. Similar concentrations of nanoparticles filling up spaces between the tetrapods can be observed in cross-sectional images near the surface and near the substrate. It is expected that such a morphology would result in an improved performance since more dye can be

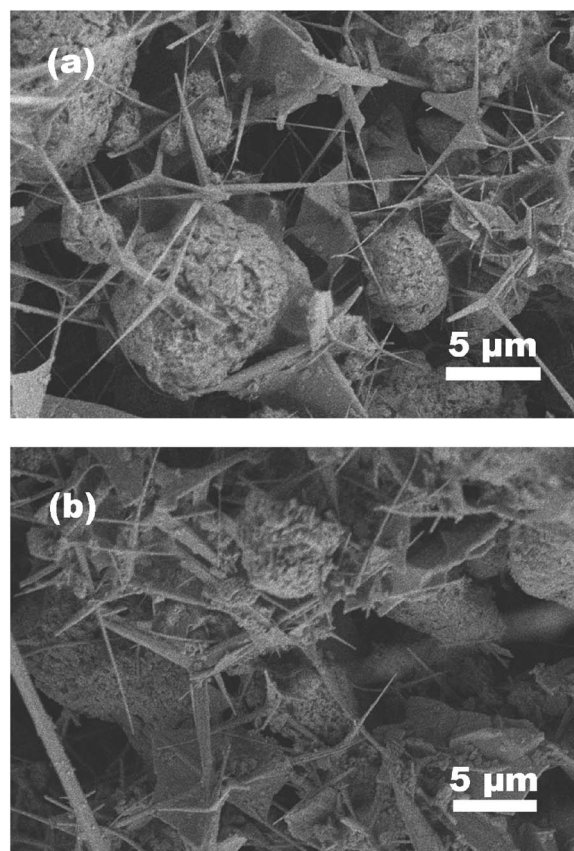


FIG. 3. Representative SEM images of the cross section of the mixed morphology film: (a) area near the substrate and (b) area near the surface.

adsorbed onto the ZnO surface, while the tetrapods still offer efficient conductive pathways for electron collection. The  $I$ - $V$  curves of the fabricated cells (for 130 and 320  $\mu\text{m}$  thicknesses) are shown in Fig. 4 and summarized in Table III. For both of the film thickness values, higher efficiencies are obtained for mixed morphology films compared to those of tetrapod only films. Similar to the effect of tetrapod film thickness increase, increase in the surface area enhanced  $J_{sc}$  but at the same time added the recombination sites and lowered FF. Although FF decreased after the addition of ZnO nanoparticles, the efficiency was still higher when compared

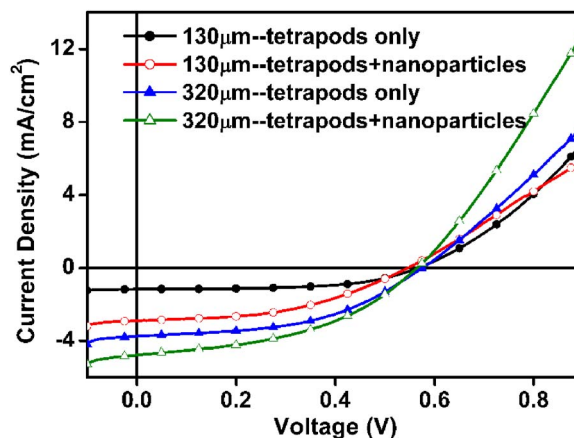


FIG. 4. (Color online) Photocurrent-voltage characteristics of cells with a mixed layer morphology at 130 and 320  $\mu\text{m}$ .

TABLE III. Performance of the cells with the addition of nanoparticles (NPs).

	Thickness ( $\mu\text{m}$ )	$J_{\text{sc}}$ (mA/cm <sup>2</sup> )	$V_{\text{oc}}$ (V)	FF	Efficiency (%)
Tetrapods only	130	1.17	0.59	0.56	0.39
Tetrapods+NPs	130	2.90	0.55	0.45	0.72
Tetrapods only	320	3.76	0.58	0.47	1.02
Tetrapods+NPs	320	4.78	0.57	0.44	1.20

to that of the film obtained by using only tetrapods. This illustrates the importance of the achievement of a large surface area to improve the efficiency of DSSCs based on morphologies different from those of nanoparticle films. Also, since the tetrapods used in this work are relatively large, other possible methods to achieve further improvements in the cell performance include the use of smaller tetrapods or a mixture of tetrapods with different sizes.

#### IV. CONCLUSION

We fabricated DSSCs by using ZnO tetrapods and studied the effects of the layer thickness and the dye used on the solar cell performance. Considering the fact that a much larger active layer thickness compared to that of a typical DSSC still resulted in a reasonable efficiency of tetrapod based cells, ZnO tetrapods represent a promising candidate for the further development of ZnO based DSSCs. Increase in the number of tetrapods enhanced the surface area for dye adsorption, resulting in improvement in the performance of the cells. It was also demonstrated that the addition of nanoparticles could further increase the efficiency. The best achieved efficiency of a tetrapod cell was 1.20% under simulated AM 1.5 global conditions.

#### ACKNOWLEDGMENTS

The work reported in this paper was supported by the Research Grants Council of The Hong Kong Special Administrative Region, China (HKU Project Nos. 7008/04P, 7010/05P, and 7019/04P). Financial support from the Strategic

Research Theme, University Development Fund, Seed Funding Grant (administrated by The University of Hong Kong), and Outstanding Young Researcher Award is also acknowledged.

- <sup>1</sup>B. O'Regan and M. Grätzel, *Nature (London)* **353**, 737 (1991).
- <sup>2</sup>M. Grätzel, *J. Photochem. Photobiol. C* **4**, 145 (2003).
- <sup>3</sup>N. Kopydakis, K. D. Benkstein, J. van de Lagemaat, and A. J. Frank, *J. Phys. Chem. B* **107**, 11307 (2003).
- <sup>4</sup>K. Y. Cheung, C. T. Yip, A. B. Djurišić, Y. H. Leung, and W. K. Chan, *Adv. Funct. Mater.* **17**, 555 (2007).
- <sup>5</sup>M. Law, L. E. Green, J. C. Johnson, R. Saykally, and P. D. Yang, *Nat. Mater.* **4**, 455 (2005).
- <sup>6</sup>K. Sayama, H. Suguhara, and H. Arakawa, *Chem. Mater.* **10**, 3825 (1998).
- <sup>7</sup>W. J. Lee, A. Suzuki, K. Imaeda, H. Okada, A. Wakahara, and A. Yoshida, *Jpn. J. Appl. Phys., Part 1* **43**, 152 (2004).
- <sup>8</sup>I. Gur, N. A. Fromer, C. P. Chen, A. G. Kanaras, and A. P. Alivisatos, *Nano Lett.* **7**, 409 (2007).
- <sup>9</sup>K. Hara, T. Horiguchi, T. Kinoshita, K. Sayama, H. Sugihara, and H. Arakawa, *Sol. Energy Mater. Sol. Cells* **64**, 115 (2000).
- <sup>10</sup>V. A. L. Roy, A. B. Djurišić, W. K. Chan, J. Gao, H. F. Lui, and C. Surya, *Appl. Phys. Lett.* **83**, 141 (2003).
- <sup>11</sup>M. Law, L. E. Greene, A. Radenovic, T. Kuykendall, J. Liphardt, and P. D. Yang, *J. Phys. Chem. B* **110**, 22652 (2006).
- <sup>12</sup>L. Y. Zeng, S. Y. Dai, W. W. Xu, and K. J. Wang, *Plasma Sources Sci. Technol.* **8**, 172 (2006).
- <sup>13</sup>K. Keis, C. Bauer, G. Boschloo, A. Hagfeldt, K. Westermark, H. Rensmo, and H. Siegbahn, *J. Photochem. Photobiol., A* **148**, 57 (2002).
- <sup>14</sup>K. Keis, E. Magnusson, H. Lindstrom, S. E. Lindquist, and A. Hagfeldt, *Sol. Energy Mater. Sol. Cells* **73**, 51 (2002).
- <sup>15</sup>A. S. Polo, M. K. Itokazu, and N. Y. M. Iha, *Coord. Chem. Rev.* **248**, 1343 (2004).
- <sup>16</sup>K. Keis, J. Lindgren, S. E. Lindquist, and A. Hagfeldt, *Langmuir* **16**, 4688 (2000).
- <sup>17</sup>J. J. Wu, G. R. Yang, C. H. Ku, and J. Y. Lai, *Appl. Phys. Lett.* **90**, 213109 (2007).